IEEE Access
Multidisciplinary | Rapid Review | Open Access Journal

Received 7 July 2023, accepted 2 August 2023, date of publication 25 August 2023, date of current version 26 September 2023.

Digital Object Identifier 10.1109/ACCESS.2023.3308816

RESEARCH ARTICLE

Energy Recovered in Exhaust Gases on Diesel Engine, Oriented to a Hybrid Drivetrain

JOSÉ MANUEL BENITEZ[1], LUIS ALVAREZ-ICAZA[2], GUILLERMO BECERRA-NUNEZ[3], ADRIÁN CAMACHO RAMÍREZ[4], AND JUAN DE ANDA[1]

[1]Tecnológico Nacional de México, ITS Purísima del Rincón, Guanajuato 36425, Mexico
[2]Instituto de Ingeniería, Universidad Nacional Autónoma de México, Coyoacán, Mexico City 04510, Mexico
[3]CONAHCYT, Universidad Autónoma del Estado de Quintana Roo, Chetumal 77019, Mexico
[4]Facultad de Ingeniería, Universidad Autónoma del Estado de México (UAEMEX), Toluca 50100, Mexico

Corresponding author: José Manuel Benitez (manuel.bq@purisima.tecnm.mx)

This work was supported by the Universidad Nacional Autónoma de México- Programa de Apoyo a Proyectos de Investigación e Innovación Tecnológica (UNAM-PAPIIT) under Grant IT1000623.

ABSTRACT In recent years, various technologies have been developed for hybrid vehicles, ranging from energy management to the type of engines used, where Diesel engines have been used with the aim to improve fuel efficiency. This work presents a novel scheme for energy recovery from the exhaust gases of a turbocharged diesel engine integrated into a hybrid powertrain. The operation is explained through simulations conducted in MATLAB, using a fifth-order dynamic model where the dynamics of the compressor and turbine are not coupled and for which a feedback linearized controller is designed. Simulation results confirm the presence of excess energy in the exhaust gases. To demonstrate this, an engine velocity profile is simulated and the available o required power in both input and output manifolds is determined. The integral of the difference between these two powers clearly identifies an energy excess that can be converted to electric energy to be used in the propulsion system. This decoupling of the compressor and turbine is crucial as in conventional turbochargers they are mechanically coupled. The implementation of this schemes requires to couple to the shaft of the turbocompresor a high speed electrical engine that absorbs the available energy excess. Finally, the achieved recovery ranges from $1-3\%$, which demonstrates the effectiveness of the proposal.

INDEX TERMS Hybrid propulsion train, diesel engine control, feedback linearized control, mathematical model, turbocharger.

NOMENCLATURE

α (radians)	Efficiency Polynomial constants.
η_{bat}	Battery charge or discharge efficiency.
η_c	Compressor isentropic efficiency.
η_t	Turbine isentropic Efficiency.
η_v	Diesel Engine volumetric efficiency.
$\mu\ (J/(kg \cdot K))$	Air specific heat ratio.
$\omega\ (rad/s)$	Diesel engine angular velocity.
$\tau_a\ (s)$	Compressor time constant.
$\tau_e\ (s)$	Turbine time constant.
λ	Compression relationship.
$c_p\ (J/(kg \cdot K))$	Specific heat at constant pressure.
$J\ (kg \cdot m^2)$	Diesel engine inertia constant.
$\dot{m}_f\ (kg/s)$	fuel flow.
$\dot{m}_{ao}\ (kg/s)$	air flow entering the combustion chamber.
n	Cylinders numbers.
$p_a, p_e\ (Pa)$	Intake and exhaust manifold pressure.
$P_a, P_e\ (W)$	Intake and exhaust manifold power.
$P_{th}\ (J/kg)$	Diesel calorific value.
$r\ (J/mol \cdot K)$	Universal ideal gas constant.
$T_a, T_e\ (K)$	Intake and exhaust manifold temperature.
$T_o\ (K)$	Environmental temperature.
$\upsilon_1\ (kg/s)$	Fuel flow.
$\upsilon_2\ (kg)$	Recirculated gas flow.
$\upsilon_3\ (kg)$	Airflow in the intake manifold.
$\upsilon_4\ (kg)$	Gas flow in the exhaust manifold.
$V_a, V_e\ (m^3)$	Intake and exhaust manifold volume.
$V_{cy}\ (m^3)$	Cylinder volume.

The associate editor coordinating the review of this manuscript and approving it for publication was Ton Duc Do.

I. INTRODUCTION

Currently, one of the globally significant problems is the reduction of polluting gases emitted by internal combustion engines. This issue leads to public health problems and contributes to global warming, among other concerns. The introduction of forced air induction by turbochargers in diesel internal combustion engines (ICE), has lead to considerable improvements in the efficiency of all types of engines [1]. This supports the reduction of environmental issues. However, with the current injection technology, forced air induction, variable camshaft timing, etc., ICEs have become more difficult to control [2]. In the literature, we can find some control techniques, such as the ones presented below. In [3], where a model-based control for a turbocharged diesel engine is used, with the principal aim of achieving the necessary torque and velocity while minimizing fuel consumption and pollutant emissions. Feedback linearization is utilized in [4], that proposes a Lyapunov function for controlling a desired angular velocity in diesel engines. In [5], a decentralized PI controller and state parametric estimation are presented for different configurations of the mass air flow sensor. A linearized model of the turbocharger around the equilibrium points is used in [6] to derive values for control design. In [7], the non-linear model and the demonstration of control by linearization are described, with the aim of regulating the angular velocity of the combustion engine.

The control of variable geometry turbocharger in a new dynamic model that considers manifold escape dynamics is analyzed in [8]. This model linearizes multiple operating points to construct an input-state controller that achieves regulation around desired velocity, manifold pressure, and power in the system. This work introduces a new configuration for the turbocompressor system in a diesel engine, assuming it is used in a hybrid powertrain. This system allows energy recovery from the exhaust gases, which in turn leads to an increase in the overall ICE efficiency. In [9], a robust and optimal design method is proposed for the engine operating area. The first proposal utilizes generalized predictive nonlinear control to handle the specific load point. The management of the motor operating point varies depending on the mentioned load point. To design this point, driving cycles and the vehicle's mass are taken into consideration. In [10], a solution is presented that combines a small displacement turbocharger Diesel with an axial flux permanent magnet electric motor in a plug-in parallel mild-hybrid powertrain. This configuration delivers the same power as a larger displacement and more powerful engine while offering the advantages of reduced emissions and fuel consumption.

The new model configuration requires separating the dynamics of the turbine and compressor. To develop the new dynamic model, the angular velocity of the crankshaft and intake manifold pressure are modeled as in [11], the dynamics of the exhaust manifold follows from [8], and the dynamics of the compressor and turbine has similarities with that presented in [12]. A preliminary version of the model was presented in [13], where the power excess between the exhaust and intake manifolds was derived for static engine speed references. The thesis in [11] also presents a fifth-order model that utilizes three driving cycles obtained from buses operating in Mexico City as references. It is demonstrated that throughout these cycles, there is an excess of power in the exhaust manifold, which can be effectively recovered as electric energy for hybrid propulsion powertrain.

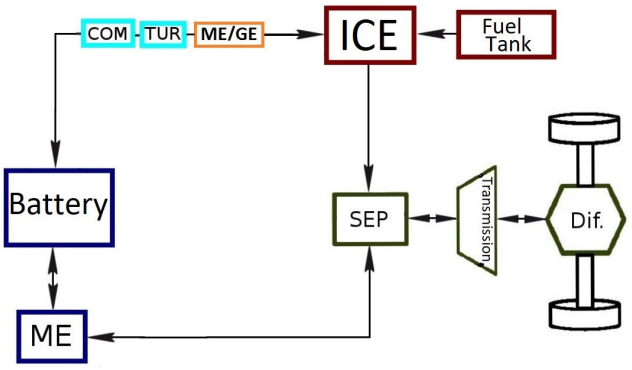

FIGURE 1. Schematic energy flow diagram.

The main objective of the present work is to describe the modeling of an internal combustion diesel engine, which features the integration of an attached electric generator with an exhaust gas-driven turbine, as well as a compressor powered by an electric motor for air supply. A control system for the entire setup is also included, along with an analysis of the amount of recovered energy. This is due to the presence of excess power between the intake and exhaust manifolds when tracking different static references. It is observed that as the engine's power demand increases, there is a corresponding increase in power in both manifolds. This results in a greater power surplus in the exhaust manifold. Consequently, the recovery of this excess power is feasible.

This article is organized as follows: Section II describes the diesel engine model, including the turbine and compressor. Section III presents the calculation of equilibrium points and their subsequent utilization as desired operation points, while Section IV details the design of the controller. Section V shows simulation results pertaining to the system's behavior. Finally, Section VI presents the conclusions of the work.

II. SYSTEM MODELING

Figure 1 shows the schematic diagram of the energy flow of the entire hybrid electric propulsion powertrain, where ME is the electric motor, SEP is the planetary gears system. COM-TUR are the compressor and turbine and ME/GE is the mechatronic device that controls and uncouples the compressor and turbine, finally Dif. is the mechanical differential on the tractor axle.

A. ENGINE VELOCITY DYNAMICS

The model formulation begins with the balance of powers to determine the engine angular velocity dynamics ω based on

the kinetic energy.

$$\frac{d}{dt}\left(\frac{1}{2}J\omega^2\right) = P_i - P_f \tag{1}$$

where, J represents the engine inertia, P_i denotes the power generated by fuel combustion, and P_f signifies the power induced by external loads, such as disturbances, wind, road conditions, etc. The expression for P_i is as follows:

$$P_i = \eta_i p_{th} \dot{m}_f \tag{2}$$

where $\dot{m}_f$ represents fuel flow, η_i represents conversion efficiency, and p_{th} calorific power. Since representing the efficiency conversion of fuel is difficult, a second-degree polynomial equation (3) is used as proposed in [7].

$$\eta_i = a_\lambda + b_\lambda \lambda + c_\lambda \lambda^2 \tag{3}$$

Using the air-fuel ratio λ,

$$\lambda = \frac{\dot{m}_{ao}}{\dot{m}_f} \tag{4}$$

where $\dot{m}_{ao}$ represents the rate of air flow entering the combustion chamber.

Solving equation (1) and using equations (2), (3) and (4) yields

$$\frac{d\omega}{dt} = \frac{1}{J\omega}\left[\left(a_\lambda + b_\lambda \frac{\dot{m}_{ao}}{\dot{m}_f} + c_\lambda \left(\frac{\dot{m}_{ao}}{\dot{m}_f}\right)^2\right) p_{th}\dot{m}_f - P_f\right] \tag{5}$$

If one assumes that the air in the intake manifold behaves as an ideal gas, neglects the heat interchange on the intake manifold walls, and assumes that the temperature varies slowly with respect to the pressure and engine velocity, then $\dot{m}_{ao}$ can be determined by,

$$\dot{m}_{ao} = \eta_v(\omega)(\dot{m}_{ao})_{th} \tag{6}$$

and

$$(\dot{m}_{ao})_{th} = \frac{nV_{cy}\omega p_a}{4\pi r T_a} \tag{7}$$

where η_v represents volumetric efficiency, V_{cy} represents the volume associated with the linear piston displacement, n is the number of cylinders, r is the universal gas constant, p_a is the pressure, and T_a is the intake manifold temperature. Using the same structure as in η_i, then η_v can be also represented by a polynomial function that depends on engine velocity [7],

$$\eta_v(\omega) = \alpha_0 + \alpha_1\omega + \alpha_2\omega^2$$

with $\alpha_0, \alpha_1 > 0$ y $\alpha_2 < 0$, by rearranging terms and correctly defining the parameters, equation (5) transforms into

$$\dot{\omega} = \epsilon_1 \frac{\upsilon_1}{\omega} + \epsilon_2 \eta_v^2 p_a + \epsilon_3 \eta_v \frac{p_a^2 \omega}{\upsilon_1} - \epsilon_4 \frac{P_f}{\omega} \tag{8}$$

where $\upsilon_1 = \dot{m}_f$ has been redefined and the rest of the defined parameters are at the end subsection C.

B. INTAKE MANIFOLD DYNAMICS

According to mass conservation law, the dynamic mass m_a on the intake manifold can be express as:

$$\frac{dm_a}{dt} = \dot{m}_{ai} - \dot{m}_{ao} \tag{9}$$

where $\dot{m}_{ai}$ is the inflow into the intake manifold and $\dot{m}_{ao}$ was defined in equation (6). The inflow to the intake manifold is expressed as [4]

$$\dot{m}_{ai} = \upsilon_2 + \upsilon_3 \tag{10}$$

where υ_2 represents the recirculation exhaust gas flow, and υ_3 is the flow coming from the compressor, where normally up to 10% of the total exhaust gases are recirculated [8].

V_a is the volume. The mass in the intake manifold satisfies:

$$m_a = \frac{p_a V_a}{r T_a} \tag{11}$$

Taking the time derivative of equation (11) and utilizing equations (6) and (9) yields

$$\frac{dp_a}{dt} = \frac{T_a r \dot{m}_{ai}}{V_a} - \frac{V_{cy} n \omega p_a}{4 V_a \pi}\eta_v$$

Finally, after replacing (10) and defining parameters properly:

$$\dot{p}_a = \epsilon_5(\upsilon_3 + \upsilon_2 - \epsilon_6 \eta_v \omega p_a) \tag{12}$$

C. EXHAUST MANIFOLD DYNAMICS

To achieve a similar mass balance in the exhaust manifold, as was done in the intake manifold [8], we can utilize the form in equation (11) to determine the output conditions in the exhaust manifold, therefore

$$\frac{dp_e}{dt}\frac{V_e}{rT_e} = \dot{m}_{eo} - \dot{m}_{ei} \tag{13}$$

where $\dot{m}_{ei}$ and $\dot{m}_{eo}$ represent the airflows entering and leaving the exhaust manifold respectively, p_e, V_e and T_e are pressure, volume and temperature in exhaust manifold. If a similar argument to the one used in the intake manifold is used, then the entry flow in the exhaust manifold can be expressed as

$$\dot{m}_{ei} = \epsilon_8 \eta_v \omega p_e + \upsilon_1 \tag{14}$$

where the injected fuel flow υ_1 added to combustion chamber is also considered. The outflow represents the flow of gases as

$$\dot{m}_{eo} = \upsilon_2 + \upsilon_4 \tag{15}$$

where υ_4 represents the flow of gases passing through the turbine. By substituting equations (14) and (15) into eq. (13), we obtain the dynamic equation for the exhaust manifold pressure.

$$\frac{V_e}{dt}\frac{dp_e}{dt} = \upsilon_2 + \upsilon_4 - \upsilon_1 - \epsilon_8 \eta_v \omega p_e \tag{16}$$

From here, the pressure dynamics in the output manifold can be expressed in the following form

$$\dot{p}_e = \epsilon_7(\upsilon_2 + \upsilon_4 - \upsilon_1 - \epsilon_8\eta_v\omega p_e) \tag{17}$$

In summary, the model parameters ϵ_1 to ϵ_8 are defined as follows:

$$\epsilon_1 = \frac{a\,pth}{J} \quad \epsilon_2 = \frac{c\,pthV_{cy}^2n^2}{16Jr^2T_a^2\pi^2} \quad \epsilon_3 = \frac{b\,pth\,V_{cy}n}{4JrT_a\pi}$$
$$\epsilon_4 = \frac{1}{J} \quad \epsilon_5 = \frac{rT_a}{V_a} \quad \epsilon_6 = \frac{nV_{cy}}{4\pi\,r\,T_a}$$
$$\epsilon_7 = \frac{rT_e}{V_e} \quad \epsilon_8 = \frac{nV_{cy}}{4\pi\,r\,T_e}$$

The values of the set of parameters were obtained from [7].

D. TURBINE AND COMPRESSOR DYNAMICS

Theoretically, the maximum power that can be delivered by the turbine depends directly on temperature T_e and the pressure p_e in the exhaust manifold. If the process is reversible and the realized work is isoentropic, the equation that describes the turbine power is:

$$P_t = k_t\left(1 - \left(\frac{p_o}{p_e}\right)^{\mu}\right) \tag{18}$$

where

$$k_t = \eta_t\upsilon_4C_pT_e$$

with η_t, the turbine efficiency; C_p the specific heat to constant pressure; and p_o, the atmospheric pressure. Lastly, $\mu = \frac{1-\gamma}{\gamma}$, where $\gamma = C_p/C_v$ and C_v represents the specific heat at constant volume.

The equation describing the power of the compressor is very similar to the turbine equation, with the difference being that the compressor requires power.

$$P_c = k_c\left(\left(\frac{p_a}{p_o}\right)^{\mu} - 1\right) \tag{19}$$

where

$$k_c = \upsilon_3C_pT_o\frac{1}{\eta_c}$$

with η_c the compressor efficiency and T_o environment temperature.

The main objective of this paper is to decouple the compressor and turbine, treating them as independent systems, and demonstrate that there is energy to be recovered in the exhaust gases. Since this is not a mechanical design issue, the article assumes that the compressor is coupled to an electric motor, which provides sufficient energy to compress the gases entering the combustion chamber. Similarly, the turbine is coupled to an electric generator, which transfers the recovered energy to the hybrid powertrain's battery bank. Assuming a stationary state, equations (18) and (19) represent the available power for operating the turbine and compressor, respectively. Consequently, the power dynamics in the intake P_{ad} and exhaust P_{es} can be represented by:

$$\dot{P}_{ad} = \frac{P_c - P_{ad}}{\tau_a}$$
$$\dot{P}_{es} = \frac{P_t - P_{es}}{\tau_e}$$

where τ_a and τ_e are time constants for the power evolution in both manifolds.

The required power compressor and the available in the turbine are rewritten as follows:

$$P_c = E_c \cdot \upsilon_3 \tag{20}$$
$$P_t = E_t \cdot \upsilon_4 \tag{21}$$

where E_c and E_t represent the specific energy for the compressor and turbine, respectively. These can be observed in equations (18) and (19) as functions of pressure and temperature in the intake and exhaust manifolds, respectively. The constants τ_a and τ_e are denote the delays in the compressor and turbine, respectively. Substituting equations (20) and (21) into (18) and (19), respectively, yields:

$$\dot{P}_{ad} = \frac{(E_c)\upsilon_3 - P_{ad}}{\tau_a} \tag{22}$$
$$\dot{P}_{es} = \frac{(E_t)\upsilon_4 - P_{es}}{\tau_e} \tag{23}$$

E. COMPLETE MODEL

By incorporating equations (8), (12), (17), (22) and (23), the complete mathematical model for the turbocharged diesel engine is obtained as:

$$\begin{aligned}
\dot{\omega} &= \epsilon_1\frac{\upsilon_1}{\omega} + \epsilon_2\eta_v^2\frac{p_a^2\omega}{\upsilon_1} + \epsilon_3\eta_v p_a - \epsilon_4\tau \\
\dot{p}_a &= \epsilon_5(\upsilon_2 + \upsilon_3 - \epsilon_6\eta_v\omega p_a) \\
\dot{p}_e &= \epsilon_7(\upsilon_2 + \upsilon_4 - \upsilon_1 - \epsilon_8\eta_v\omega p_e) \\
\dot{P}_{ad} &= \frac{(E_c)\upsilon_3 - P_{ad}}{\tau_a} \\
\dot{P}_{es} &= \frac{(E_t)\upsilon_4 - P_{es}}{\tau_e}
\end{aligned} \tag{24}$$

III. EQUILIBRIUM POINTS

Equilibrium points are obtained by setting the dynamic equations of the system equal to zero, i.e.

$$\begin{aligned}
0 &= \epsilon_1\frac{\bar{\upsilon}_1}{\bar{\omega}} + \epsilon_2\eta_v^2\frac{\bar{p}_a^2\bar{\omega}}{\upsilon_1} + \epsilon_3\bar{p}_a - \epsilon_4\bar{\tau} \\
0 &= \epsilon_5(\bar{\upsilon}_2 + \bar{\upsilon}_3 - \epsilon_6\eta_v\bar{\omega}\bar{p}_a) \\
0 &= \epsilon_7(\epsilon_8\eta_v\bar{\omega}\bar{p}_e + \bar{\upsilon}_1 - \bar{\upsilon}_2 - \bar{\upsilon}_4) \\
0 &= (E_c)\bar{\upsilon}_3 - \bar{P}_{ad} \\
0 &= (E_t)\bar{\upsilon}_4 - \bar{P}_{es}
\end{aligned} \tag{25}$$

To obtain an algebraic system from five equations and ten unknowns, we consider the controls υ_i and the load torque τ as unknowns. In the following, the notation $\bar{\cdot}$ denotes a feasible solution for the corresponding variable in the equations

(25). To solve the system, we propose fixing four variables: $\bar{\omega}$, $\bar{\tau}$, $\bar{\lambda}$ and $\bar{F}_{egr}$. The last variable corresponds to the fraction of exhaust gases that are recirculated to the intake manifold. The desired air flow in the compressor, $\bar{\upsilon}_3$, is obtained from the air-fuel ratio, $\bar{\lambda}$, and the fraction of recirculated gases, $\bar{F}_{egr}$, as proposed in [4].

$$\begin{aligned}\bar{\upsilon}_3 = \frac{\bar{\upsilon}_1}{2}(&\bar{\lambda}(1-\bar{F}_{egr}+15.6\bar{F}_{egr}-1+\\&+((\bar{\lambda}(1-\bar{F}_{egr})+15.6\bar{F}_{egr})^2+\\&+4(1-\bar{F}_{egr})\bar{\lambda})^{\frac{1}{2}})\end{aligned} \tag{26}$$

The recirculation exhaust gases flow to the intake manifold, $\bar{\upsilon}_2$, can be calculated as a fraction of $\bar{F}_{egr}$, as described in [8]

$$\bar{\upsilon}_2 = \frac{\bar{F}_{egr}}{1-\bar{F}_{egr}}\bar{\upsilon}_3 \tag{27}$$

To obtain the value $\bar{\upsilon}_1$, as defined in (26), the auxiliary variable W_e is used as follows:

$$\begin{aligned}W_E = \frac{1}{2}(&\bar{\lambda}(1-\bar{F}_{egr})+15.6\bar{F}_{egr}-1+\\&+((\bar{\lambda}(1-\bar{F}_{egr}+15.6\bar{F}_{egr}-1)^2+\\&+4(1-\bar{F}_{egr})\bar{\lambda})^{\frac{1}{2}})\end{aligned}$$

Similarly, in (27), FE is defined as follows:

$$FE = \frac{\bar{F}_{egr}}{1-\bar{F}_{egr}}$$

These variables, $\bar{\upsilon}_2$, $\bar{\upsilon}_3$ and $\bar{\upsilon}_4$ can be described as:

$$\bar{\upsilon}_2 = \bar{\upsilon}_1 \cdot FE \cdot W_E \tag{28}$$
$$\bar{\upsilon}_3 = \bar{\upsilon}_1 \cdot W_E \tag{29}$$
$$\bar{\upsilon}_4 = \bar{\upsilon}_3 + \bar{\upsilon}_1 \tag{30}$$

Additionally, $\bar{p}_a$ from (25) is

$$\bar{p}_a = \frac{\bar{\upsilon}_2 + \bar{\upsilon}_3}{\epsilon_6 \bar{\omega}} \tag{31}$$

Substitute (31) into (25) to get

$$\bar{\omega} = \frac{1}{\epsilon_4 \tau}\left(\epsilon_1 \bar{\upsilon}_1 + \epsilon_2 \eta_v^2 \frac{(\bar{\upsilon}_2+\bar{\upsilon}_3)^2}{\epsilon_6^2 \bar{\upsilon}_1} + \epsilon_3 \eta_v \frac{\bar{\upsilon}_2+\bar{\upsilon}_3}{\epsilon_6}\right) \tag{32}$$

Then substitute (28) and (29) and factorize $\bar{\upsilon}_1$ in (32) to obtain

$$\bar{\omega} = \bar{\upsilon}_1\left(\frac{\epsilon_1 h_6^2 + \epsilon_2 \eta_v^2 (\Lambda W_E)^2 + \epsilon_3 \eta_v \epsilon_6 \eta_v \Lambda W_E}{\epsilon_4 \tau h_6^2 \eta_v^2}\right) \tag{33}$$

Finally, $\bar{\upsilon}_1$ is solved for in equation (33)

$$\bar{\upsilon}_1 = \frac{\bar{\omega}\epsilon_4 \tau h_6^2 \eta_v^2}{\epsilon_1 h_6^2 \eta_v^2 + \epsilon_2 \eta_v^2 (\Lambda W_E)^2 + \epsilon_3 \eta_v \epsilon_6 \eta_v \Lambda W_E} \tag{34}$$

where $\Lambda = (1 + FE)$.
With $\bar{\upsilon}_1$, it is possible to obtain $\bar{\upsilon}_2$, $\bar{\upsilon}_3$, $\bar{\upsilon}_4$ from (28)-(30).

The known value of $\bar{\upsilon}_i$ is substituted into the other equations, starting with (31)

$$\bar{p}_a = \frac{(\bar{\upsilon}_2+\bar{\upsilon}_3)(\epsilon_4\epsilon_6\eta_v\tau\bar{\upsilon}_1)}{\Lambda_0 + \epsilon_2\eta_v^2(\bar{\upsilon}_2+\bar{\upsilon}_3)^2} \tag{35}$$

where $\Lambda_0 = (\epsilon_6\eta_v\bar{\upsilon}_1)(\epsilon_1\epsilon_6\eta_v\bar{\upsilon}_1 + \epsilon_3\eta_v(\bar{\upsilon}_2+\bar{\upsilon}_3))$

Use (19), (20) and (31) in (26) to obtain

$$\bar{P}_c = k_c\left[\left(\frac{\sigma_1}{p_o(\sigma_2\sigma_3+\sigma_4)}\right)^{\mu} - 1\right] \tag{36}$$

where

$$\begin{aligned}k_c &= C_p T_a \frac{1}{\eta_c}\\ \sigma_1 &= (\bar{\upsilon}_2+\bar{\upsilon}_3)(\epsilon_4\epsilon_6\eta_v\tau\bar{\upsilon}_1)\\ \sigma_2 &= \epsilon_6\eta_v\bar{\upsilon}_1\\ \sigma_3 &= \epsilon_1\epsilon_6\eta_v\bar{\upsilon}_1 + \epsilon_3\eta_v(\bar{\upsilon}_2+\bar{\upsilon}_3)\\ \sigma_4 &= \epsilon_2\eta_v^2(\bar{\upsilon}_2+\bar{\upsilon}_3)^2\end{aligned}$$

and

$$\bar{p}_e = \frac{\bar{\upsilon}_2 + \bar{\upsilon}_4 - \bar{\upsilon}_1}{\epsilon_8\eta_v\bar{\omega}} \tag{37}$$

Substituting $\bar{\omega}$ from (32) yields

$$\bar{p}_e = \frac{(\bar{\upsilon}_2+\bar{\upsilon}_4-\bar{\upsilon}_1)(\epsilon_4\epsilon_6^2\eta_v^2\bar{\upsilon}_1\tau)}{\epsilon_1\epsilon_6^2\eta_v^2\epsilon_8\eta_v\bar{\upsilon}_1^2 + \epsilon_2\epsilon_4\epsilon_8\bar{\tau}(\bar{\upsilon}_2+\bar{\upsilon}_3)^2 + \sigma_5} \tag{38}$$

where $\sigma_5 = \epsilon_3\eta_v\epsilon_4\epsilon_6\eta_v\epsilon_8\eta_v\tau\bar{\upsilon}_1(\bar{\upsilon}_2+\bar{\upsilon}_3)$. Similarly to (26)

$$\bar{P}_t = \bar{k}_t\left[1 - \left(\frac{p_o(\sigma_6+\sigma_7+\sigma_8)}{(\sigma_9)(\sigma_{10})}\right)^{\mu}\right] \tag{39}$$

with

$$\begin{aligned}\bar{k}_t &= \bar{\upsilon}_4 C_p \eta_t T_e\\ \sigma_6 &= \epsilon_1\epsilon_6^2\eta_v^2\epsilon_8\eta_v\bar{\upsilon}_1^2\\ \sigma_7 &= \epsilon_2\eta_v^2\epsilon_4\epsilon_8\eta_v\bar{\tau}(\bar{\upsilon}_2+\bar{\upsilon}_3)^2\\ \sigma_8 &= \epsilon_3\eta_v\epsilon_4\epsilon_6\eta_v\epsilon_8\eta_v\bar{\tau}\bar{\upsilon}_1(\bar{\upsilon}_2+\bar{\upsilon}_3)\\ \sigma_9 &= \bar{\upsilon}_2+\bar{\upsilon}_4-\bar{\upsilon}_1\\ \sigma_{10} &= \epsilon_4\epsilon_6^2\eta_v^2\bar{\upsilon}_1\bar{\tau}\end{aligned}$$

A. EQUILIBRIUM POINTS SET

$$\begin{aligned}\bar{\omega} &= \frac{1}{\epsilon_4\bar{\tau}}\left(\epsilon_1\bar{\upsilon}_1 + \epsilon_2\eta_v^2\frac{(\bar{\upsilon}_2+\bar{\upsilon}_3)^2}{\epsilon_6^2\eta_v^2\bar{\upsilon}_1} + \epsilon_3\eta_v\frac{\bar{\upsilon}_2+\bar{\upsilon}_3}{\epsilon_6\eta_v}\right)\\ \bar{p}_a &= \frac{(\bar{\upsilon}_2+\bar{\upsilon}_3)(\epsilon_4\epsilon_6\eta_v\bar{\tau}\bar{\upsilon}_1)}{\Lambda_0 + \epsilon_2\eta_v^2(\bar{\upsilon}_2+\bar{\upsilon}_3)^2}\\ \bar{p}_e &= \frac{(\bar{\upsilon}_2+\bar{\upsilon}_4-\bar{\upsilon}_1)(\epsilon_4\epsilon_6^2\eta_v^2\bar{\upsilon}_1\bar{\tau})}{\epsilon_1\epsilon_6^2\eta_v^2\epsilon_8\eta_v\bar{\upsilon}_1^2 + \epsilon_2\eta_v^2\epsilon_4\epsilon_8\eta_v\bar{\tau}(\bar{\upsilon}_2+\bar{\upsilon}_3)^2 + \sigma_5}\\ \bar{P}_c &= k_c\left[\left(\frac{\sigma_1}{p_o(\sigma_2\sigma_3+\sigma_4)}\right)^{\mu} - 1\right]\\ \bar{P}_t &= k_t\left[1 - \left(\frac{p_o(\sigma_6+\sigma_7+\sigma_8)}{(\sigma_9)(\sigma_{10})}\right)^{\mu}\right]\end{aligned} \tag{40}$$

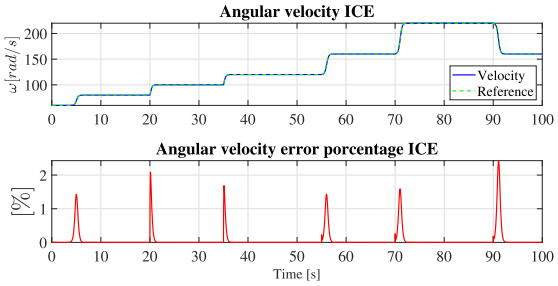

FIGURE 2. Angular velocity and tracking error.

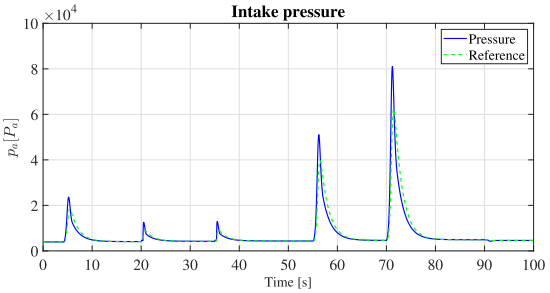

FIGURE 3. Compressor pressure.

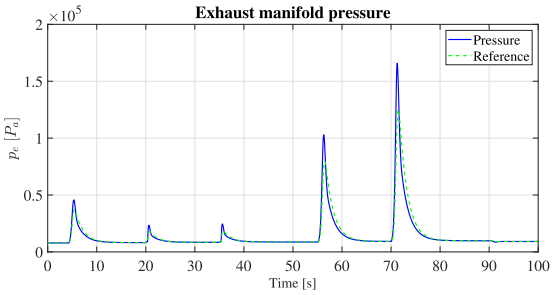

FIGURE 4. Turbine pressure.

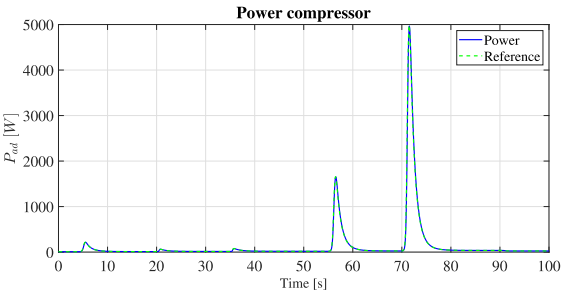

FIGURE 5. Intake power compressor.

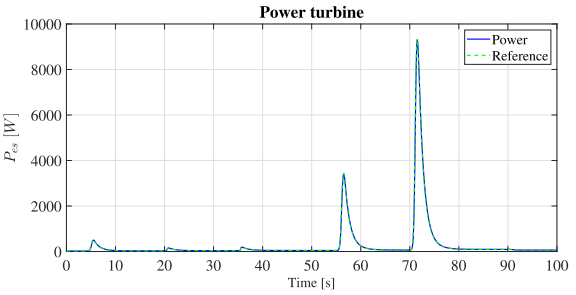

FIGURE 6. Exhaust power turbine.

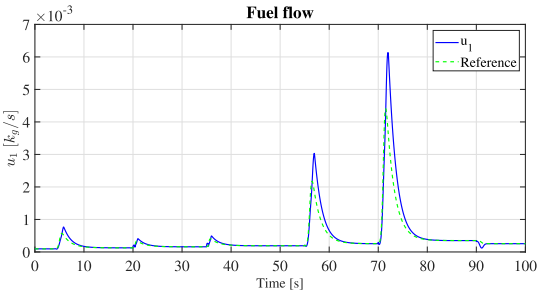

FIGURE 7. Fuel flow.

IV. CONTROLLER OF THE TURBOCHARGED DIESEL ENGINE

It is necessary to design a controller that ensures convergences to the system trajectories at the calculated equilibrium points from the previous section. To achieve this, a similar process is followed as proposed by [7] and [14] for designing a controller using state-feedback linearization for a fifth-order dynamic system.

The following outputs for system (24) are proposed to construct the controller

$$y_1 = \omega \tag{41}$$

$$y_2 = \frac{p_e}{\epsilon_7} - \frac{p_a}{\epsilon_5} \tag{42}$$

$$y_3 = P_{ad} \tag{43}$$

$$y_4 = P_{es} \tag{44}$$

Rewriting the output in error terms, where $i = 1, 2, 3, 4$

$$\tilde{y}_i = y_i - \bar{y}_i \tag{45}$$

where $\bar{y}_i$ are the outputs obtained by substituting the equilibrium points found in the previous section.

Starting with equation (45) where $i = 1$ and deriving it with respect to time yields

$$\dot{\tilde{y}}_1 = \dot{y}_1 - \dot{\bar{y}}_1 \tag{46}$$

Following the methodology proposed in [7] and [14] for static-feedback, the control for υ_1 is proposed in such a way that the closed-loop system exhibits a linear structure, with respect to the gain k_1

$$\dot{\tilde{y}}_1 = \epsilon_1 \frac{\upsilon_1}{\omega} + \epsilon_2 \eta_v^2 \frac{p_a^2 \omega}{\upsilon_1} + \epsilon_3 \eta_v p_a - \epsilon_4 \tau = -k_1 \tilde{y}_1 \tag{47}$$

By rearranging equation (47), the control signal υ_1 is obtained:

$$\upsilon_1 = \frac{-\psi_1 + \sqrt{(\psi_1)^2 - 4(\epsilon_1/\omega)(\epsilon_2)\eta_v^2 p_a^2)}}{2\epsilon_1/\omega} \tag{48}$$

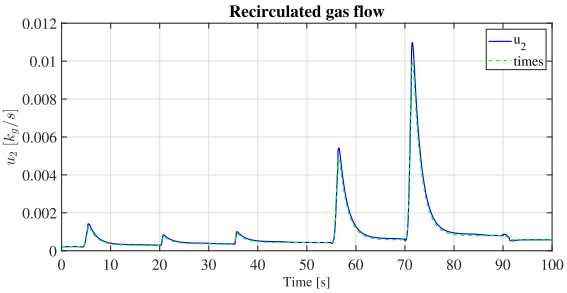

FIGURE 8. EGR flow.

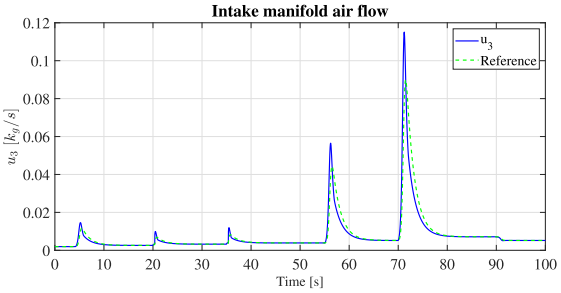

FIGURE 9. Intake manifold air flow.

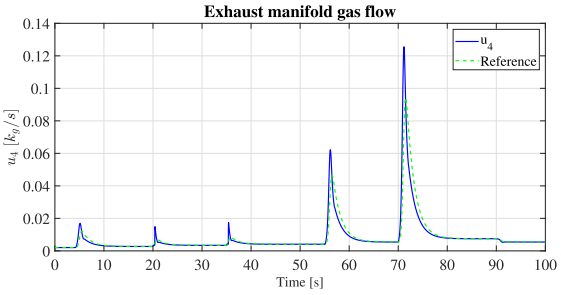

FIGURE 10. Exhaust manifold gas flow.

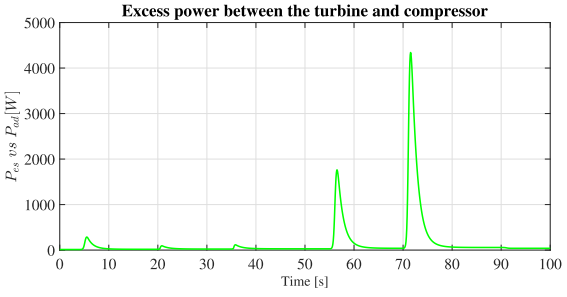

FIGURE 11. Power difference between exhaust and intake manifolds.

Here, $\psi_1 = (\epsilon_3\eta_v p_a - \epsilon_4\tau + k_1\tilde{y}_1)$ and the control is valid if and only if $\upsilon_1 > 0$, $\omega > 0$, and $k_1 > 0$.
To design the signal control for υ_2, equation (45) is used with $i = 2$, and derived with respect to time

$$\dot{\tilde{y}}_2 = \upsilon_4 - \upsilon_1 - \epsilon_8\eta_v\omega p_e - \upsilon_3 + \epsilon_6\eta_v\omega p_a = -k_2\tilde{y}_2 - k_3\dot{\tilde{y}}_2 \tag{49}$$

It can be observed that the control does not appear in this first derivative, which was already expected because the

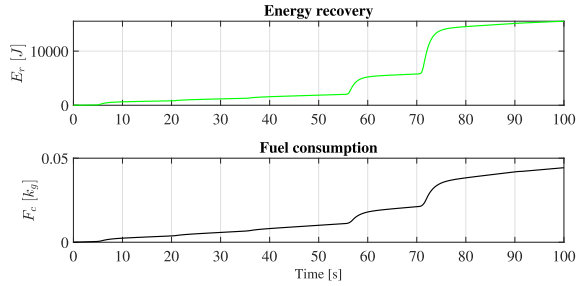

FIGURE 12. Recovered energy and fuel consumption.

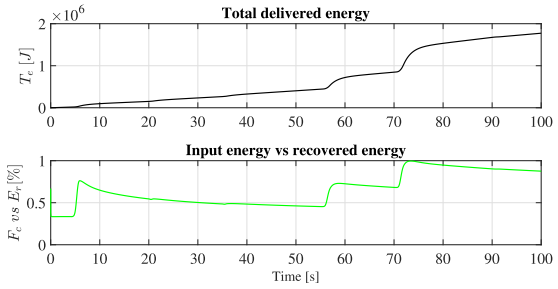

FIGURE 13. Total energy delivered and recovered percentage.

chosen output has relative degree of two. Therefore, equation (49) is derived again with respect to time to obtain

$$\ddot{\tilde{y}}_2 = \psi_2 + \psi_3 + \psi_4 - \psi_5 + \psi_6 \tag{50}$$

where $\psi_2 = -\upsilon_1 + ((\epsilon_1\upsilon_1/\omega)$, $\psi_3 = ((\epsilon_2\omega\eta_v^2 p_a^2)/\upsilon_1) + \epsilon_3\eta_v p_a - \epsilon_4\tau)(\epsilon_6\eta_v p_a - \epsilon_8\eta_v p_e)$, $\psi_4 = \omega\epsilon_6\eta_v\epsilon_5(\upsilon_3 - \epsilon_6\eta_v\omega p_a)$, $\psi_5 = \omega\epsilon_7\epsilon_8\eta_v(\upsilon_4 - \upsilon_1 - \epsilon_8\eta_v\omega p_e)$ and $\psi_6 = \upsilon_2(\omega(\epsilon_6\eta_v\epsilon_5 - \epsilon_7\epsilon_8\eta_v))$.

After taking the second derivative, the control signal υ_2 appears, confirming the relative degree of the system. The control signal υ_2 is calculated from:

$$\upsilon_2 = \frac{\dot{\upsilon}_1 - (\kappa_1 + \kappa_2 + \kappa_3)(\kappa_4) - \kappa_5 + \kappa_6 - k_2\dot{\tilde{y}}_2 - k_3\ddot{\tilde{y}}_2}{(\kappa_7)} \tag{51}$$

where $\kappa_1 = (\epsilon_1\kappa_1/\omega)$, $\kappa_2 = (\epsilon_2\omega\eta_v^2 p_1^2)/\kappa_1$, $\kappa_3 = \epsilon_3\eta_v p_1 - \epsilon_4\tau$, $\kappa_4 = \epsilon_6\eta_v p_1 - \epsilon_8\eta_v p_2$, $\kappa_5 = \omega\epsilon_6 n\eta_v\epsilon_5(\upsilon_3 - \epsilon_6\eta_v\omega p_1)$, $\kappa_6 = \omega\epsilon_7\epsilon_8\eta_v\cdot(\upsilon_4 - \upsilon_1 - \epsilon_8\eta_v\omega p_2)$, $\Upsilon_7 = \omega(\epsilon_6\eta_v\epsilon_5 - \epsilon_7\epsilon_8\eta_v$, $k_2 > 0$ and $k_3 > 0$. Now, use the equation (45) with $i = 3$ to obtain the control signal υ_3, which is then derived with respect to time.

$$\dot{\tilde{y}}_3 = E_c\upsilon_3 - P_{ad} = -k_4\tilde{y}_3 \tag{52}$$

from where control signal υ_3 is

$$\upsilon_3 = \frac{P_{ad} - k_4\tilde{y}_3}{E_c} \tag{53}$$

The dynamic equations of the turbine and compressor exhibit great similarity to each other. In obtaining the control signal υ_4, the methodology used to find υ_3 is reproduced,

$$\dot{\tilde{y}}_4 = E_t\upsilon_4 - P_{es} = -k_4\tilde{y}_4 \tag{54}$$

Using equation (45) with $i = 4$ yields:

$$\upsilon_4 = \frac{P_{es} - k_5 \tilde{y}_4}{E_t} \tag{55}$$

with $k_4 > 0$ and $k_5 > 0$.

It should be noted that three out of the four outputs have a relative degree of one, while the remaining output has a relative degree of two. The total relative degree of the system is five, indicating the absence of zero dynamics. The terms $\bar{y}_i$ represent system references, calculated based on the equilibrium conditions presented in the previous section. This selection ensures exponential stability, as $y_i - \bar{y}_i = 0$.

V. SIMULATIONS

The controller was tested using a 10% gas recirculation fraction, an air-fuel ratio of 40, and a simulation sampling time of 0.1ms [8]. The proposed controller for the new ICE achieved good results, which can be observed in the following figures.

Figure 2 shows the tracking of a representative piecewise constant speed reference ω rad/s. The tracking error remains very small and smaller that 2% int the step angular velocity changes, for all ranges of velocities.

Close to idle speed, the model remains valid when the electric motor is engaged to meet the power demand of the hybrid electric vehicle. The behavior of the other states involved in this model, such as the pressures in the intake and exhaust manifolds, is illustrated in figures 3 and 4. As expected, step changes in velocity produce a transient behavior with a relatively small settling time.

The power on the compressor and turbine (5 and 6) are monitored. The states are compared to the previously constructed references, which were established in Section III. It can be observed that sudden changes in the reference velocity result in transients in the pressure and power signals, but these are quickly dampened by the designed controller. The first group of simulations was conducted using a stepped velocity profile as an initial test to assess the reliability of the control.

The next set of figures displays the variables that were used as control inputs. These variables include fuel flow 7, recirculation gases flow 8, intake manifold air flow 9, and gases exhaust manifold flow 10. that are shown in figures 7-10, respectively.

Figure 11 illustrates the power difference between the exhaust and intake manifolds, with the intake manifold consuming power and the exhaust manifold delivering it. The figure depicts the available power that can be utilized.

Finally, figure 12 depicts the recovered energy and fuel consumption, while figure 13 presents the relationship between the delivered energy and the recovered energy in percentage terms.

VI. CONCLUSION

In this work, a new fifth-order mathematical model was presented for a turbocharged diesel engine that incorporates an electric machine directly coupled to the turbocharger shaft. This fifth-order model allows for decoupling of the compressor and turbine dynamics. The model was developed to show the feasibility of energy recovering from the exhaust gases.

While the focus of the exhaust gas energy recovery system, as mentioned earlier, is on hybrid propulsion systems, no power distribution tests were conducted between the internal combustion engine (ICE) and the electric machine in this study. The static feedback controller used demonstrates good state tracking, although some peaks observed in the simulations are a result of sudden changes in the angular velocity reference for the motor. These peaks can be mitigated by using saturated controls and smoother references, which are commonly used in driving cycles.

During the simulation tests, a segment of a drive cycle was employed that explores typical operating speeds of a diesel engine. The results showed good tracking of engine speed, recirculated exhaust gas fraction, and air-fuel ratio, even in the presence of sudden changes in the applied load torque. More importantly, simulation results signal that overall engine recovering reaches up to 1% of the total energy content of the supplied fuel. Considering the ICE efficiency ranges, this is equivalent to an increase close to 3%. More energy is recovered with more aggressive driving cycles. If the speed is constant, the recovery is not significant.

Implementation of this strategy in a hybrid powertrain is ongoing work, as well as the analysis of other control strategies.

REFERENCES

[1] K. Mollenhauer and H. Tschoke, *Handbook of Diesel Engine*. Cham, Switzerland: Springer, 2010.

[2] J. Heywood, *Internal Combustion Engine Fundamentals*. New York, NY, USA: McGraw-Hill, 1988.

[3] L. Guzzella and A. Amstutz, "Control of diesel engines," *IEEE Control Syst.*, vol. 18, no. 5, pp. 53–71, Oct. 1998.

[4] M. Jankovic, M. Jankovic, and I. Kolmanovsky, "Constructive Lyapunov control design for turbocharged diesel engines," *IEEE Trans. Control Syst. Technol.*, vol. 8, no. 2, pp. 288–299, Mar. 2000.

[5] M. van Nieuwstadt, I. Kolmanovsky, P. Moraal, and M. Jankovic, "EGR-VGT control schemes: Experimental comparison for a high-speed diesel engine," *IEEE Control Syst. Mag.*, vol. 20, no. 3, pp. 63–79, Jun. 2000.

[6] D. Ambuhl, O. Sundstrom, A. Sciarreta, and L. Guzzella, "Explicit optimal control policy and its practical application for hybrid electric powertrains," *Control Eng. Pract.*, vol. 18, no. 12, pp. 1429–1939, 2010.

[7] R. Outbib, X. Dovifaaz, A. Rachid, and M. Ouladsine, "A theoretical control strategy for a diesel engine," *J. Dyn. Syst., Meas., Control*, vol. 128, no. 2, pp. 453–457, Jun. 2006.

[8] J. L. Mendoza, "Control de un sistema híbrido diesel-eléctrico," Ph.D. dissertation, Instituto de Ingeniería, Universidad Nacional Autónoma de México, Coyoacán, Mexico, 2013.

[9] Y. Liu, Q. Sun, Q. Han, H. Xu, W. Han, and H.-Q. Guo, "A robust design method for optimal engine operating zone design of plug-in hybrid electric bus," *IEEE Access*, vol. 10, pp. 6978–6988, 2022.

[10] B. Anton and A. Florescu, "Design and development of series-hybrid automotive powertrains," *IEEE Access*, vol. 8, pp. 226026–226041, 2020.

[11] J. M. Benitez, "Regeneración de energía en gases de escape en un motor diésel," Ph.D. dissertation, Instituto de Ingeniería, Universidad Nacional Autónoma de México, Coyoacán, Mexico, 2021.

[12] K. Rong, "Modeling of turbocharged spark ignited engine and model predictive control of a turbocharger," Ph.D. dissertation, Herbert Wertheim College Eng. Mech., Univ. Florida, Gainesville, FL, USA, 2014.

[13] M. Benitez and L. Alvarez-Icaza, "Recuperación de energía en gases de escape de motores diésel," in *Proc. Memorias del Congreso Nacional de Control Automático*, Oct. 2017, pp. 415–420.

[14] H. Rodríguez, A. Astolfi, and R. Ortega, "On the construction of static stabilizers and static output trackers for dynamically linearizable systems, related results and applications," *Int. J. Control*, vol. 79, no. 12, pp. 1523–1537, Dec. 2006.

JOSÉ MANUEL BENITEZ received the B.S. degree in mechatronic engineer from the Technological Institute of Toluca, and the master's and Ph.D. degrees in electrical engineering from Universidad Nacional Autónoma de México (UNAM). He is currently a Full-Time Professor in Automotive Engineering Division, TecNM-Superior de Purísima del Rincón. His research interests include robotics, mechatronics, AI and control systems.

LUIS ALVAREZ-ICAZA received the B.S. degree in mechanical engineering and the master's degree in control engineering from Universidad Nacional Autónoma de México (UNAM), and the Ph.D. degree in mechanical from Berkeley California. He is a Researcher with UNAM. Moreover, he is a National Researcher with SNI. His research interests include control theory and modeling and identification of electro-mechanical systems.

GUILLERMO BECERRA-NUNEZ received the M.S. and Ph.D. degrees in (control) electrical engineering from UNAM, in 2010 and 2015, respectively. He is currently a Professor with Universidad Autónoma del Estado de Quintana Roo, Chetumal, Mexico, commissioned by CONAHCYT. He is a National Researcher with SNI. His research interests include nonlinear control theory, mechatronics, optimal control, and applications.

ADRIÁN CAMACHO RAMÍREZ received the master's degree in electrical engineering from Universidad Nacional Autónoma de México (UNAM) and the Ph.D. degree from Universidad Autónoma del Estado de México (UAEMEX). He is a Mechatronic Engineer with the Technological Institute of Toluca. His research interests are robotics and control systems.

JUAN DE ANDA received the B.Sc. degree in physics from the University of Guanajuato, in 2012, the M.Sc. degree in computer science from TecNM–de León, in 2014, and the Ph.D. degree in computer science from TecNM–de Tijuana, in 2019. He is currently a full-time Professor with the Electromechanical Engineering Division, TecNM—Superior de Purísima del Rincón. His research interests include estimation of distribution algorithms, information theory, and computational physics. He is a member of the National System of Researchers of the National Council of Humanities Science and Technology of Mexico (SNI-CONAHCYT).